mice with yttrium-90-labeled anti-Ly1 monoclonal antibody: therapy of the T cell lymphoma EL4. *Cancer Res* 1991;51:1883–1890.
6. Deshpande SV, DeNardo SJ, Meares CF, et al. Copper-67-labeled monoclonal antibody Lym-1, a potential radiopharmaceutical for cancer therapy: labeling and biodistribution in RAJI tumored mice. *J Nucl Med* 1988;29:217–225.
7. Beaumier PL, Venkatesan P, Vanderheyden JL, et al. ^{86}Re radioimmunotherapy of small cell lung carcinoma xenografts in nude mice. *Cancer Res* 1991;51:676–681.
8. Schlom J, Siler K, Milenic DE, et al. Monoclonal antibody-based therapy of a human tumor xenograft with a ^{77}lutetium-labeled immunoconjugate. *Cancer Res* 1991;51: 2889–2896.
9. Kozak RW, Atcher RW, Gansow OA, Friedman AM, Hines JJ, Waldmann TA. Bismuth-212-labeled anti-Tac monoclonal antibody: alpha-particle-emitting radionuclides as modalities for radioimmunotherapy. *Proc Natl Acad Sci USA* 1986;83:474–478.
10. Zalutsky MR, Garg PK, Friedman HS, Bigner DD. Labeling monoclonal antibodies and F(ab') fragments with the alpha-particle-emitting nuclide astatine-211: preservation of immunoreactivity and in vivo localizing capacity. *Proc Natl Acad Sci USA* 1989;86:7149–7153.
11. Martell AE, Smith RM. *Critical stability constants. Amino acids*, vol. 1. New York: Plenum Press; 1974:281–284.
12. Chinol M, Hnatowich DJ. Generator-produced yttrium-90 for radioimmunotherapy. *J Nucl Med* 1987;28:1465–1470.
13. Wessels BW, Rogus RD. Radionuclide selection and model absorbed dose calculations for radiolabeled tumor associated antibodies. *Med Phys* 1984;11:638–645.
14. Klein JL, Nguyen TH, Laroque P, et al. Yttrium-90 and iodine-131 radioimmunoglobulin therapy of an experimental human hepatoma. *Cancer Res* 1989;49:6383–6389.
15. Juweid M, Neumann R, Paik C, et al. Micropharmacology of monoclonal antibodies in solid tumors: direct experimental evidence for a binding site barrier. *Cancer Res* 1992;52:5144–5153.
16. Saga T, Neumann RD, Heya T, et al. Targeting cancer micrometastases with monoclonal antibodies: a binding-site barrier. *Proc Natl Acad Sci USA* 1995;92:8999–9003.
17. Stewart JS, Hird V, Snook D, et al. Intraperitoneal yttrium-90-labeled monoclonal antibody in ovarian cancer. *J Clin Oncol* 1990;8:1941–1950.
18. Stewart JS, Hird V, Snook D, et al. Intraperitoneal radioimmunotherapy for ovarian cancer: pharmacokinetics, toxicity, and efficacy of I-131 labeled monoclonal antibodies. *Int J Radiat Oncol Biol Phys* 1989;16:405–413.
19. Hnatowich DJ, Virzi F, Doherty PW. DTPA-coupled antibodies labeled with yttrium-90. *J Nucl Med* 1985;26:503–509.
20. Roselli M, Schlom J, Gansow OA, et al. Comparative biodistributions of yttrium- and indium-labeled monoclonal antibody B72.3 in athymic mice bearing human colon carcinoma xenografts. *J Nucl Med* 1989;30:672–682.
21. Brechbiel MW, Gansow OA, Atcher RW, et al. Synthesis of 1-(p-isothiocyanatobenzyl) derivatives of DTPA and EDTA. Antibody labeling and tumor-imaging studies. *Inorg Chem* 1986;25:2772–2781.
22. Kozak RW, Raubitschek A, Mirzadeh S, et al. Nature of the bifunctional chelating agent used for radioimmunotherapy with yttrium-90 monoclonal antibodies: critical factors in determining in vivo survival and organ toxicity. *Cancer Res* 1989;49:2639–2644.
23. Sharkey RM, Motta-Hennessy C, Gansow OA, et al. Selection of a DTPA chelate conjugate for monoclonal antibody targeting to a human colonic tumor in nude mice. *Int J Cancer* 1990;46:79–85.
24. Washburn LC, Sun TT, Lee YC, et al. Comparison of five bifunctional chelate techniques for ^{90}Y-labeled monoclonal antibody CO17-1A. *Int J Radiat Appl Instrum B* 1991;18:313–321.
25. Deshpande SV, Subramanian R, McCall MJ, DeNardo SJ, DeNardo GL, Meares CF. Metabolism of indium chelates attached to monoclonal antibody: minimal transchelation of indium from benzyl-EDTA chelate in vivo. *J Nucl Med* 1990;31:218–224.
26. Harrison A, Walker CA, Parker D, et al. The in vivo release of ^{90}Y from cyclic and acyclic ligand–antibody conjugates. *Int J Radiat Appl Instrum B* 1991;18:469–476.
27. Watanabe N, Goodwin DA, Meares CF, et al. Immunogenicity in rabbits and mice of an antibody-chelate conjugate: comparison of (S) and (R) macrocyclic enantiomers and an acyclic chelating agent. *Cancer Res* 1994;54:1049–1054.
28. Kosmas C, Snook D, Gooden CS, et al. Development of humoral immune responses against a macrocyclic chelating agent (DOTA) in cancer patients receiving radioimmunoconjugates for imaging and therapy. *Cancer Res* 1992;52:904–911.
29. Kosmas C, Maraveyas A, Gooden CS, Snook D, Epenetos AA. Anti-chelate antibodies after intraperitoneal yttrium-90-labeled monoclonal antibody immunoconjugates for ovarian cancer therapy. *J Nucl Med* 1995;36:746–753.
30. Kodama M, Koike T, Mahatma AB, Kimura E. Thermodynamic and kinetic studies of lanthanide complexes of 1,4,7,10,13-pentaazacyclopentadecane-N, N', N'',N''',N''', hexaacetic acid. *Inorg Chem* 1991;30:1270–1273.
31. Camera L, Kinuya S, Garmestani K, et al. Evaluation of the serum stability and in vivo biodistribution of CHX-DTPA and other ligands for yttrium labeling of monoclonal antibodies. *J Nucl Med* 1994;35:882–889.
32. Brechbiel MW, Gansow OA. Synthesis of C-functionalized trans-cyclohexyldiethylenetriaminepentaacetic acids for labelling of monoclonal antibodies with the bismuth-212 α-particle emitter. *J Chem Soc Perkin Trans* 1992;1:1173–1178.
33. Pastan I, Lovelace ET, Gallo MG, Rutherford AV, Magnani JL, Willingham MC. Characterization of monoclonal antibodies B1 and B3 that react with mucinous adenocarcinomas. *Cancer Res* 1991;51:3781–3787.
34. Mirzadeh S, Brechbiel MW, Atcher RW, Gansow OA. Radiometal labeling of immunoproteins: covalent linkage of 2-(4-isothiocyanatobenzyl) diethylenetriaminepentaacetic acid ligands to immunoglobulin. *Bioconjug Chem* 1990;1:59–65.
35. Wu C, Kobayashi H, Sun B-F, et al. Stereochemical influence on the stability of radio-metal complexes in vivo. Synthesis and evaluation of the four stereoisomers of 2-(*p*-nitrobenzyl)-*trans*-CyDTPA. *Bioorg Med Chem* 1997;5:1925–1934.
36. Pippin CG, Parker TA, McMurry TJ, Brechbiel MW. Spectrophotometric method for the determination of a bifunctional DTPA ligand in DTPA-monoclonal antibody conjugates. *Bioconjug Chem* 1992;3:342–345.
37. Greenwood FC, Hunter WM, Glover JS. The preparation of ^{131}I-labelled human growth hormone of high specific radioactivity. *Biochem J* 1963;89:114–123.
38. Camera L, Kinuya S, Pai LH, et al. Preclinical evaluation of ^{111}In-labeled B3 monoclonal antibody: biodistribution and imaging studies in nude mice bearing human epidermoid carcinoma xenografts. *Cancer Res* 1993;53:2834–2839.
39. Lindmo T, Boven E, Cuttitta F, Fedorko J, Bunn PA Jr. Determination of the immunoreactive fraction of radiolabeled monoclonal antibodies by linear extrapolation to binding at infinite antigen excess. *J Immunol Methods* 1984;72:77–89.
40. Jowsey J, Rowland RE, Marshall JH. The deposition of rare earths in bone. *Radiat Res* 1958;8:490–501.
41. Madsen SL, Bannochie CJ, Martell AE, Mathias CJ, Welch MJ. Investigation of physicochemical and in-vivo behavior of diastereomeric iron-59, gallium-68, and indium-111-EHPG trivalent metal complexes. *J Nucl Med* 1990;31:1662–1668.

Divalent Cobalt as a Label to Study Lymphocyte Distribution Using PET and SPECT

Jakob Korf, Lammy Veenma-van der Duin, Rikje Brinkman-Medema, Anita Niemarkt and Lou F.M.H. de Leij

Department of Biological Psychiatry, Groningen School of Behaviour and Cognitive Neurosciences, Groningen, and Clinical Immunology, Groningen School of Drug Exploration, University Hospital, Groningen, the Netherlands

PET and SPECT allow the study of the distribution of lymphocytes in living humans, provided that these cells are adequately prelabeled ex vivo. Such a labeling technique should not only be nontoxic to lymphocytes but it also should take into consideration that their kinetics are such that radioactivity must be followed for at least 24 hr. We describe the potential of divalent cobalt isotopes ($^{55}Co^{2+}$, half-life 17.5 hr for PET; $^{57}Co^{2+}$, half-life 270 days for SPECT) for labeling lymphocytes. **Methods:** Isolated rat lymphocytes were incubated with $^{57}CoCl_2$ with or without unlabeled $CoCl_2$ or $CaCl_2$ carrier or other compounds. In some experiments, the accumulation of radioactive cobalt and calcium in lymphocytes was determined in the presence of phorbol myristate acetate alone, calcimycine alone or in combination. The toxicity of cobalt to lymphocytes was assessed with the trypan blue exclusion test and by assessing their proliferative capacity using radioactive thymidine incorporation as a readout. Biodistribution of cobalt-labeled lymphocytes was determined with postmortem analysis and compared with that of the free (nonlymphocyte-bound) tracer. **Results:** At high concentrations (more than 100 × necessary for adequate labeling), cobalt was not cytotoxic. Incubation of labeled lymphocytes in tissue culture medium for 24 hr in vitro showed a loss of less than half of the incorporated cobalt radioactivity. Twenty-four hours after in vitro labeling of lymphocytes and intravenous injection, radioactivity accumulated not only in the liver, kidney and bladder of the rat but in the spleen and lungs, which differed from the distribution of the free tracer. Uptake and binding to rat lymphocytes of Co^{2+} partly mimicked that of Ca^{2+}. The binding of cobalt, however, was stronger and nonsaturable. **Conclusion:** These results warrant further exploration of cobalt as a PET or SPECT label of human lymphocytes.

Key Words: lymphocytes; cobalt; PET; SPECT; calcium

J Nucl Med 1998; 39:836–841

Received Apr. 1, 1997; revision accepted Aug. 6, 1997.

For correspondence or reprints contact: Jakob Korf, PhD, Department of Biological Psychiatry and Neuro-PET Coordination, Groningen University Hospital, P.O. Box 30.001, 9700 RB Groningen, the Netherlands.

The in vivo location and distribution of lymphocytes or a subpopulation of lymphocytes may be assessed quantitatively with PET or semiquantitatively with SPECT after radiolabeling ex vivo. Such an approach allows the study of the behavior of particular subsets of lymphocytes under normal conditions or during disease (*1–12*). Visualization of lymphocyte distribution with SPECT and PET is particularly informative to detect small targets in deeper structures of the body such as the central nervous system, as compared with, for example, scintigraphic planar images. In addition, PET allows quantification of the regional behavior of the tracer. Therefore, for several types of inflammation, PET and SPECT may be informative of the course of diseases both in central and peripheral tissue, including multiple sclerosis, arthritis, stroke, AIDS, trauma, tumors and organ transplantation. Mature lymphocytes recirculate continuously, going from blood to tissue and vice versa once or twice daily (*2–4*). It has been shown that intravenously injected ex vivo labeled lymphocytes accumulated first in the lungs, before their clearance starting at 3–4 hr up to 24 hr (*4,5*). To be useful for clinical applications, the labeling of lymphocytes should be nontoxic (causing neither radiation nor pharmacological damage of proliferating lymphocytes), and the label must be preferentially retained for longer periods of time (e.g., 24 hr).

Leukocyte labeling (*13–18*) is now a routine procedure in SPECT using ^{111}In-oxine (half-life 67.2 hr) or ^{99m}Tc-hexamethylpropylene amine oxime (^{99m}Tc-HMPAO) (half-life 6.02 hr), but in this way only a small fraction of lymphocytes are labeled so the sensitivity of these methods is too low or the physical half-lives of the radionuclides are too short for studies exceeding 24 hr. SPECT methods have been described to label lymphocytes specifically with ^{111}In-oxine or ^{99m}Tc-HMPAO (*5,6*). The conclusion of these studies was that at a low dose, ^{111}In-oxine was the most suitable, but not optimal, because the label was not well retained over longer periods of time. Attempts to provide leukocytes—whose fraction includes lymphocytes—with a label suitable for PET have recently been reported (*6,19*). In these reports, an ex vivo method was used with the short-lived isotopes ^{11}C and ^{18}F (physical half-lives of 20 and 110 min, respectively). Therefore, trafficking the distribution of the labeled cells in vivo can be visualized only within a few hours after their intravenous reintroduction. Such a narrow time window is too short to visualize lymphocyte distribution. An alternative labeling strategy aiming to visualize localization rather than distribution of lymphocytes in vivo is based on the use of labeled antibodies against lymphocytes. This approach has been used with the anti-T lymphocyte ^{99m}Tc-labeled antibody OKT-3 in rheumatoid arthritis; the cytotoxic properties of this antibody, however, limit widespread clinical application (*7*). Several of these limitations can be avoided by using longer lived radionuclides suitable for PET or SPECT to label isolated lymphocytes ex vivo.

We previously explored the clinical usefulness of $^{57}Co^{2+}$ and $^{55}Co^{2+}$, a single-photon and a positron-emitting radionuclide with physical half-lives of 270 days and 17.5 hr, respectively. When injected as a free divalent cation, the radionuclide was found to accumulate in damaged or inflamed brain tissue, where radioactivity remained present for several days. Accordingly, brain infarcts, trauma and relatively hot spots in multiple sclerosis—presumably reflecting inflammatory processes—were visualized (*20–27*). We also established the dosimetry of both labels with whole-body PET in humans and tissue distribution studies in rats (*28*).

This study was done to document the binding of divalent cobalt to purified lymphocytes and the behavior of the labeled cells in the rat. We also tested whether calcium and cobalt would share the same uptake mechanisms in lymphocytes by studying the separate or combined effects of phorbol-12-myristate-13 acetate (PMA; to stimulate intracellular calcium metabolism through activation of protein kinase carbon) (*1*) and calcimycine (a calcium ionophore) (*29*) on the uptake of divalent cations by lymphocytes in vitro.

MATERIALS AND METHODS

Reagents and Solutions

All reagents were of analytical grade and purchased from Merck Darmstadt (Darmstadt, Germany) unless otherwise indicated. The Krebs-Ringer HEPES buffer contained (millimolar) 125 NaCl, 5 KCl, 1.2 KH_2PO_4, 1.2 $MgSO_4.7H_2O$; 0.15–0.75 $CaCl_2.2H_2O$; 6 glucose; 25 HEPES; from 0.1% to 1% bovine serum albumin (BSA). RPMI-1640 (Bio-Whittaker, Verviers, Belgium) was used for lymphocyte washing. RPMI-1640 supplemented with 10% heat-inactivated fetal calf serum (Hyclone) and antibodies were used as a culture medium to a concentration as indicated below. The following mitogens were used: phytohemagglutinin at 5 or 10 μg/ml (PHA5 and PHA10, respectively; Murex Biotech Ltd., Dartford, Kent, UK), JJ319 (an antibody against rat CD28) in combination with R73 (an antibody against the T cell antigen receptor) were diluted in tissue culture medium (HyClone)/2 m*M* glutamine (Sigma, St. Louis, MO) allowing maximal T cell stimulation (about 0.5–1 μg/ml). In some experiments, nonradioactive $CoCl_2$ or 160 n*M* PMA (Sigma) or 1 μ*M* calcimycine (calcium ionophore A23187; Sigma) were added. In other experiments, an excess of Mg ($MgCl_2$, 6.2 m*M*), combined with EGTA (0.4 m*M*) were applied to study the influence of calcium in the medium on the uptake and binding of radioactive calcium or cobalt to lymphocytes. The radioactive compounds $^{57}CoCl_2$ and $^{45}CaCl_2$ (half-life 180 days) were obtained from Amersham (Slough, UK).

Lymphocytes

Lymphocytes were isolated from the spleens of male and female Wistar rats (weight 150 g) by gentle disruption of the tissue with a bent injection needle. After sedimentation of large tissue fragments, the lymphocytes were gently washed with RPMI 1640 medium (Bio-Whittaker)/5% heat-inactivated fetal calf serum (HyClone)/2 m*M* glutamine (Sigma). In some experiments, two or three lymphocyte suspensions were combined, centrifuged (20 min at 1000 g on Isopacque/Ficoll, density 1.076), carefully collected, mixed with saline and centrifuged (10 min at 600 g), after which the pellet was resuspended in saline (1 ml) and re-centrifuged. A small portion was resuspended in isotonic saline and counted (Coulter counter). The rest of the pellet was resuspended in Krebs-Ringer HEPES buffer to a final concentration of 4.5×10^6 cells/ml.

Toxicity

The toxicity of cobalt on lymphocytes was determined after 60 min incubation in the presence of various concentrations of $COCl_2$. The trypan blue exclusion viability test and the lymphocyte transformation test (LTT) were used to assess the viability.

In the trypan blue exclusion test, the relative proportion of nonstained cells and trypan blue-stained cells was counted. The LTT was as follows: to 50 μl mitogen solution (PHA or antibodies) a suspension of 50×10^3 rat lymphocytes in 50 μl culture medium was added. The mitogens were diluted from stock solutions (0.1 mg/ml); the concentrations in culture medium per well were 5 and 10 μg/ml for PHA and 0.5–1 μg/ml for JJ319 + R73. After 3 days of culture, 25 μl medium containing 18.5 MBq (0.5 μCi) [^{3}H]thymidine was added to each well for an additional 16 hr. Cells were harvested onto glass fiber filters, and [^{3}H]thymidine incorporation

was determined in a liquid scintillation counter. As a control, similarly isolated and treated lymphocytes, but not exposed to $CoCl_2$, were used. In the LTT, $CoCl_2$ was added to the culture medium. Viability is expressed as the percentage of viable or responsive cells in any or both the toxicity tests and compared with appropriate controls.

Cobalt Uptake

Most experiments were done in suspensions of the lymphocytes in Krebs-Ringer HEPES buffer (pH 7.4) containing 0.15 m*M* $CaCl_2$ and 0.1% BSA sterilized by filtration, except in a few cases in which other concentrations of calcium were used, as indicated. About 4.5×10^6 cells (in 1 ml) in sterile 10-ml polypropylene tubes were incubated for 15–60 min at 37°C. In the initial experiments, when incubation parameters were optimized, $^{57}CoCl_2$ (about 74 MBq [2 μCi] per tube) was added to a 1-ml cell suspension. In later experiments, when a maximal labeling was to be obtained, the 1-ml cell suspension was centrifuged (10 min at 1200 rpm), carefully decanted and 6 μl of the $^{57}CoCl_2$ were added to each tube. When incubated at minimal volumes, after the incubation 1 ml buffer was added and the cells were transferred to 50-ml tubes. After centrifugation (20 min at 1200 rpm) the supernatant was decanted and the cells resuspended in 1 ml buffer. The cells labeled with about 185 MBq (5 μCi) ^{57}Co were injected into the tail vein of a male Wistar rat (200–250 g) to determine the biodistribution.

In Vivo Distribution Studies

Twenty-four hours after injection of the labeled lymphocyte suspension, the rats were killed by decapitation under pentobarbital anesthesia. The blood was collected in heparinized tubes and the liver, kidney, lung, heart, spleen and brain were removed. In other rats, the biodistribution of free divalent ^{57}Co was studied in a similar way. These procedures were essentially as previously described (*28*). Tissue was weighed and the radioactivity determined in a well counter (Wallac 1282; Wallac Oy, Turku, Finland). The radioactivity was expressed relative to that in blood, serum or heart. To compare the distribution of free and lymphocyte-bound radioactivity, we chose the heart as the tissue of reference instead of blood because the distribution of radioactivity over cells, proteins and unbound fraction differed in the blood compartment, obviously due to the different labeling procedures. Moreover, in vivo, the relative labeling of various organs may be more important to allow visualization of the label than the low blood levels of radioactivity of either procedure. However, our conclusions about the distribution of radioactivity in the body did not depend on the choice of reference tissue or blood.

RESULTS

In Vitro Cobalt Binding and Toxicity

The time course of the incubation indicated that there was an almost linear accumulation over about 2 hr (Fig. 1). For convenience, we chose in subsequent experiments an incubation time of 30 min. In the presence of increasing concentrations of cold $CoCl_2$, the accumulation of radioactive cobalt declined at higher concentrations with an apparent half maximal effect at 3 μmol (Fig. 2, top) when the same data were used to determine the absolute amount of cobalt accumulated in the lymphocytes, a virtually linear relationship with cobalt in the medium emerged, as shown in the bottom of Figure 2.

On the basis of the results obtained with the trypan blue exclusion test, more than 93 ± 3% of the lymphocytes (n = 6, s.e.m.) remained viable at concentrations of cobalt up to 1 m*M*, which is far beyond the concentrations of divalent cobalt used in the radiolabeling experiments. When incubated for 3 days only at the high concentration of 10 μM $CoCl_2$, the incorporation of [^{3}H]thymidine diminished (Table 1). The addition of any concentration of cobalt according to the same procedure used for labeling did not affect viability. In the LTT, essentially no inhibition of [^{3}H]thymidine incorporation in DNA (103 ± 4; mean and s.e.m. three experiments) was found at cobalt

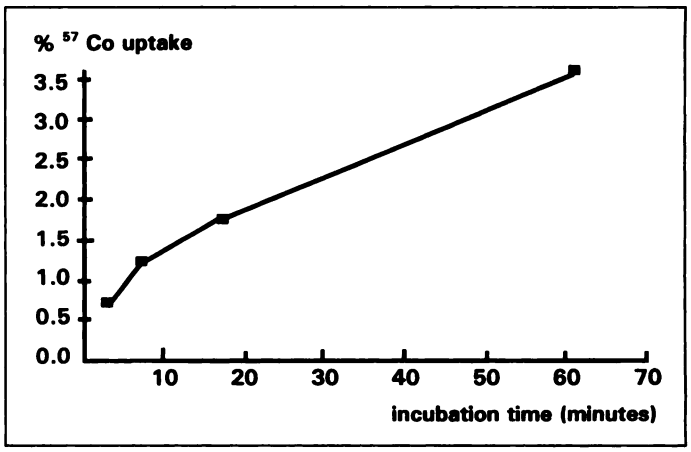

FIGURE 1. Time course of accumulation of radioactive cobalt in lymphocytes. Expressed are the percentage of radioactivity bound to cells as compared with that in the medium. Note that lymphocytes are incubated in 1 ml buffered medium. Mean of three experiments. The s.e.m. is within the squares.

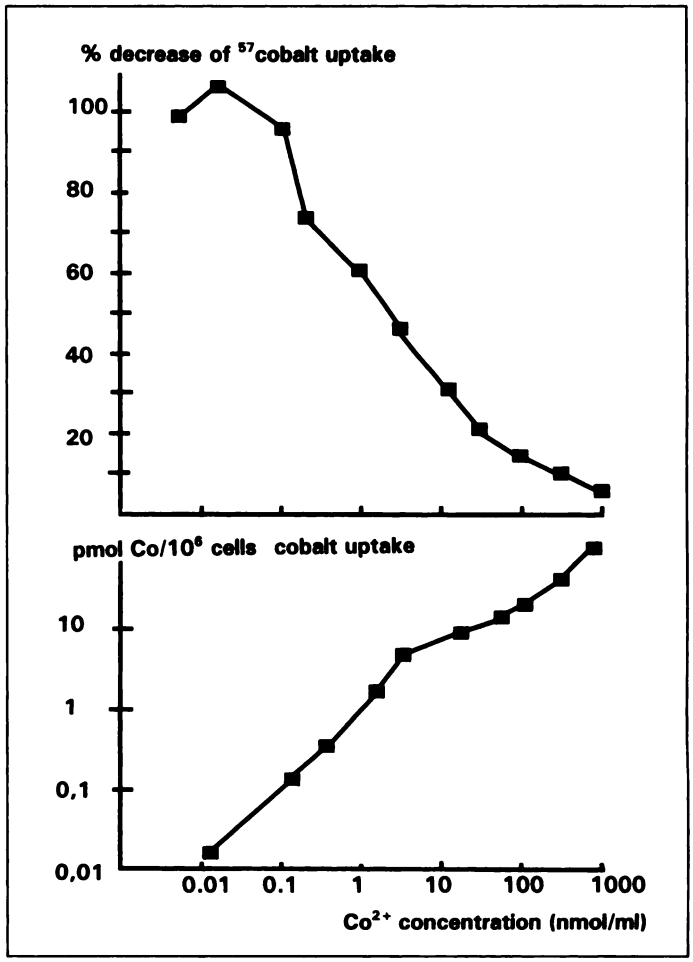

FIGURE 2. Uptake of the tracer ^{57}Co (top half) and the absolute amount of divalent cobalt (bottom half) after incubation of lymphocytes for 30 min under the same conditions as described in Figure 1. The radioactivity is expressed as the percentage when only ^{57}Co was present; the absolute amount of cobalt was derived from the top half of the graph by taking into account the decreasing specific activity at increasing divalent cobalt concentrations (carrier). There is only a weak saturable part in the curve below 10 nmol/liter.

TABLE 1
[^{3}H]Tritium-Labeled Thymidine Incorporation with Increasing $CoCl_2$ Concentration in Culture Medium

Concentration	PHA5 (%)	PHA10 (%)	αCD28/αCD3 (%)
No $CoCl_2$ added	100 ± 2	100 ± 5	100 ± 45
0.1 μM $CoCl_2$	104 ± 9	88 ± 2	142 ± 73
1 μM $CoCl_2$	76 ± 14	65 ± 6	131 ± 41
10 μM $CoCl_2$	23 ± 0.4	24 ± 7	102 ± 16

[^{3}H]thymidine radioactivity of lymphocytes cultured for 3 days in a medium containing the indicated concentrations $CoCl_2$ in the presence of the indicated mitogens compared with cobalt-free medium (mean ± s.e.m.; the number of experiments was three per $CoCl_2$/mitogen).

concentrations up to 1.5 μM (Fig. 3). We noticed, however, that this isolation procedure had an adverse effect on viability, as tested with LTT, with about 25%.

Distribution In Vivo

Lymphocytes were incubated in a minimal volume (about 6 μl $^{57}CoCl_2$ were added to 5×10^6 cells) for 60 min, washed and injected into the tail vein of rats. The dose was 179.08 ± 34.78 MBq (4.84 ± 0.94 μCi; s.e.m., six rats). The distribution of radioactivity was determined 24 hr later. The results shown in Figure 4 indicate a major uptake of radioactivity (expressed per milligram of tissue) in the spleen, followed by the liver, lung and kidney. The uptake per organ was as follows: In the spleen 1.5 ± 0.11% of the injected radioactivity accumulated, whereas in the liver 16.7 ± 2.1% (s.e.m., six rats) and in the lungs 0.67 ± 0.05% (s.e.m., six rats) of the dose (s.e.m., six observations) were present 24 hr after injection. This pattern of distribution differed from that observed when the label was injected as free cobalt. In these experiments, radioactivity (expressed per milligram of tissue) was found predominantly in the liver and kidney (Fig. 4). With either label, little uptake was observed in the adrenal glands, brain or bone of the skull (not shown).

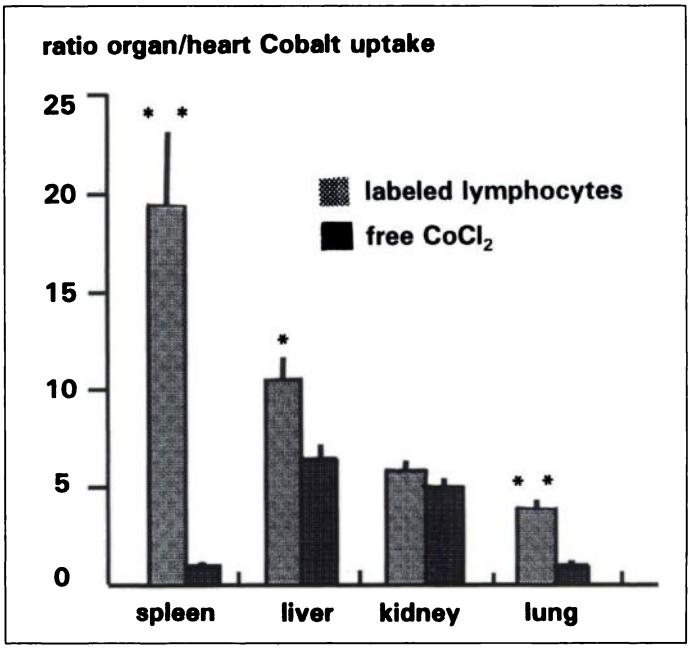

FIGURE 4. Biodistribution of radioactive lymphocytes (24 hr after labeling with ^{57}Co in a small volume and intravenous reintroduction) and of free $^{57}CoCl_2$. Note the significant differences in the spleen and lung. Bars ± s.e.m. of six or seven experiments. **p < 0.01; *p < 0.05 free versus lymphocyte cobalt.

Comparison with Calcium

Incubation of lymphocytes for 15 min in a calcium- or cobalt-containing medium resulted in a 30-fold proportionally higher labeling of the lymphocytes with ^{57}Co than with ^{45}Ca. Results are shown in Figure 5. Incubation in the presence of

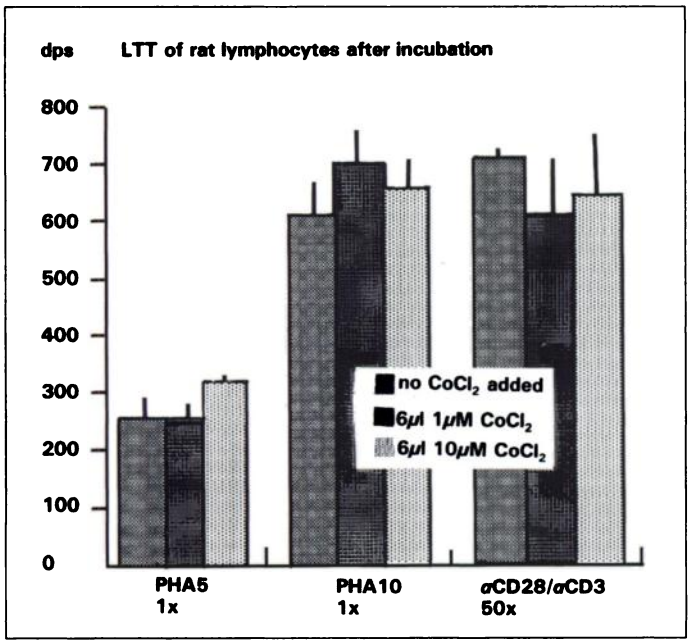

FIGURE 3. LTT: Relative toxicity of cobalt with the mitogens phytohemagglutinin at 5 or 10 μg/ml (PHA5 and PHA10) or JJ319 in combination with R73 (αCD28/αCD3). Dps: [^{3}H] radioactivity as the result of the incorporation of radioactive thymidine per 5×10^4 lymphocytes. Various amounts of cobalt were added essentially as in the experiments of Figure 2. Values are the mean ± s.e.m. (three experiments).

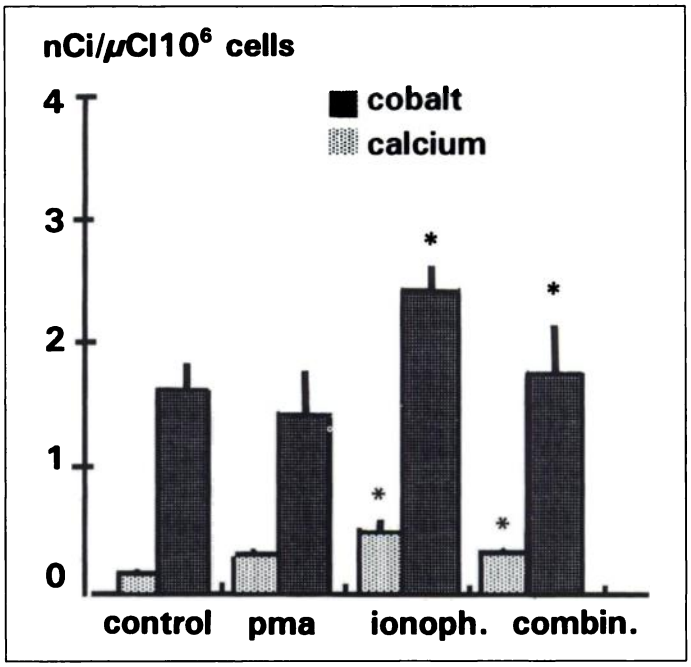

FIGURE 5. Association of radioactivity of cobalt or calcium to lymphocytes in the presence of PMA, calcimycine (calcium ionophore) alone or combined. Experimental conditions are the same as in Figure 2. In all the experiments, significantly more radioactive cobalt was bound to the lymphocytes ($p < 0.002$). In the presence of the calcium ionophore (with or without PMA), more cobalt or calcium was bound to the lymphocytes. The y-axis indicates the radioactivity relative to that in the medium per 10^6 cells. The number of observations was six (bars ± s.e.m.). $p < 0.02$.

TABLE 2
Influence of Calcium Concentration on the Labeling of Lymphocytes with Radioactive Calcium or Cobalt

Incubation	^{45}Ca with calcium	^{45}Ca without calcium	^{57}Co with calcium	^{57}Co without calcium
0.15 m*M* calcium	0.50 ± 0.03	0.82 ± 0.14	16.87 ± 0.53	16.30 ± 0.26
6.2 m*M* Mg^{2+}	0.45 ± 0.04	0.64 ± 0.03	15.36 ± 0.10	14.63 ± 0.44
6.2 m*M* Mg^{2+} 0.4 mM EGTA	0.42 ± 0.02	0.62 ± 0.07	11.09 ± 0.52*	6.20 ± 0.09*

*$p < 0.0007$ compared with cobalt labeling in the presence of magnesium or calcium only.

During loading of lymphocytes with ^{45}Ca or ^{57}Co, incubation media with various concentrations of $CaCl_2$ or $MgCl_2$ and EGTA were used as indicated. With or without calcium indicates the presence or absence of 0.5 mM $CaCl_2$. In all conditions, the binding of radioactive cobalt was far stronger than that of calcium. Except when EGTA and magnesium were combined, there was no significant effect on the binding of either label to lymphocytes. Values are expressed as the percentage of labeling of 10^6 lymphocytes of the added radioactivity of 1 ml medium (± s.e.m. of six experiments). EGTA = egtazic acid.

PMA did not influence the labeling, whereas with the calcium ionophore, more radioactivity accumulated in the lymphocytes with either isotope. In absolute terms, the net increased uptake of cobalt was about threefold that of calcium, although the relative effect of the ionophore on the uptake of cobalt radioactivity was modest. When PMA and the ionophore were combined, less radioactivity was accumulated with either tracer. In the absence of calcium in the medium, but with an excess of 6.2 m*M* Mg, more calcium accumulated, whereas the effects on cobalt binding were minimal. When all calcium was removed from the medium by EGTA and with an excess of Mg, the binding of calcium still was increased, but the accumulation of radioactive cobalt now was significantly decreased (Table 2).

DISCUSSION

Results of this study show that divalent cobalt may serve as a label to visualize and quantify the distribution of lymphocytes in vivo over periods for more than 24 hr with PET or SPECT. Here we focus on methodological aspects as determined with rat lymphocytes; human lymphocytes are discussed later. A particularly attractive feature is the low toxicity of the label. Therefore, in the acute-exposure experiments, which were similar to those used in the labeling procedure of the lymphocytes, no toxic effects of cobalt were observed. When cobalt was added during lymphocyte culture for 3 days, only at the highest concentration of cobalt toxicity was observed. It should be considered that because of the nearly linear accumulation of cobalt over several hours, large amounts of cobalt were accumulated by the lymphocytes in the latter experimental condition. In addition to the labeling described here, divalent ^{60}Co also may be used for autoradiographic localization studies in animals (^{60}Co is a predominantly beta emitter −99%- maximal energy 0.314 MeV, half-life 5.27 yr). Previously, we assessed the dosimetry of free $^{55}Co^{2+}$ and $^{57}Co^{2+}$ using whole-body PET and distribution studies in rats (*27*). For Class II studies, as defined by the World Health Organization, the dose has to be limited to 18.5 MBq (0.5 mCi) and 11 MBq (0.3 mCi) of ^{55}Co and ^{57}Co, respectively. In view of the distribution of the free and the lymphocyte-bound cobalt in the rat, a similar dosimetry can be expected in humans (perhaps except in the spleen). Therefore, if the uptake of the label in inflamed tissue is of a similar order of magnitude with either free or lymphocyte-bound cobalt, the maximally allowed dose should be sufficient for visualization with PET or SPECT.

A major argument to choose divalent cobalt as a label is its similarity to calcium in several cellular processes as tested in vitro. For instance, in neurons, the uptake of divalent cobalt can be stimulated by excitatory amino acids and analogs through specific calcium channels. Moreover, it may serve as a competitive inhibitor of calcium uptake in these and other cells. The uptake of calcium in leukocytes, including lymphocytes, can be increased by calcium ionophores such as calcimycine. Intracellular calcium accumulation is enhanced by PMA, particularly through the release of the cation from endoplasmic reticulum. We showed that the uptake of radioactive cobalt was increased by the calcium ionophore as well, but that PMA alone did not affect the uptake of either cation. In combination with the ionophore, PMA decreased the relative accumulation of both cations, which again emphasized the similar behavior of the cations in this preparation. It was also clear, however, that the binding of cobalt to lymphocytes was more than ten times that of calcium, both at baseline and stimulated conditions. In fact, the relative amount of radioactive cobalt entering the lymphocytes through the ionophore was more than three times that of the calcium. Cobalt may bind to a variety of proteins, partly nonspecifically to mercapto-moieties and, alternatively, specifically to calcium channels and transferrins. Under our in vitro conditions, albumin was present, which might have limited the amount of free divalent cobalt. Considering that the major component was the nonspecific binding (Fig. 2), we assume that most of the radioactive cobalt was adsorbed at the surface of the lymphocytes and that only a small proportion was subject to cellular uptake. The latter was substantially increased by the introduction of a calcium ionophore. Our observations indicate that cobalt uptake and binding to lymphocytes is both similar to and different from that of calcium.

The in vivo distribution of the radioactive lymphocytes as compared with divalent cobalt administered in the free form was highly different. The significantly higher uptake of the label in the spleen and the lungs is consistent with the notion that a substantial proportion of radioactive cobalt still is attached to the lymphocytes in vivo 24 hr after ex vivo labeling. The biodistribution of cobalt radioactivity is similar to that of leukocytes labeled with SPECT labels, such as ^{111}In-oxine or ^{99m}Tc-HMPAO (*5,6,16,18*).

We emphasize that the free cations of both calcium and cobalt bind rapidly to proteins, possibly transferrins and albumin, once administered intravenously. To improve the labeling procedure ionophores may be used, but thus far we have been reluctant to use this approach because of the toxicity and the obstacles encountered trying to obtain permission for their clinical use. Another way to improve the labeling of lymphocytes may be to use complexed cobalt instead of free cobalt. Given the affinity of cobalt for proteins and compounds with free mercapto groups, such an approach may well be feasible for clinical applications. Alternative procedures for labeling leukocytes using ^{11}C-methylation or FDG uptake have been published (*19,30*). Of these labels, the methylation was preferred because of the stability of the label. Radioactive FDG diffuses out of the lymphocytes in vitro with a half-life of about 4 hr (Kroesen BJ, *personal communication*, 1995) and is thus not well suited to monitor lymphocyte distribution for longer

periods. Neither label allows one to monitor cells for 24 hr or longer.

If the present approach appears to be successful in human lymphocytes, the procedure will allow study of immunological responses in identifying rejection after organ transplantation, in tumor infiltration of lymphocytes during interleukin-2 treatments (*31*) and in identifying various lymphocyte-mediated central or peripheral inflammatory reactions (*32–34*). Such scanning could be helpful to optimize transplantation procedures, to suppress rejection or to slow down the progression of autoimmune diseases by early drug intervention (*1,8–12*).

CONCLUSION

In view of the known dosimetry and the low toxicity of cobalt, substantial amounts of radioactivity can be accumulated in lymphocytes. Our approach has the potential to become a highly sensitive method for in vivo study of lymphocyte distribution in humans.

ACKNOWLEDGMENTS

We thank Mrs. J. Venema and Mrs. A. de Wolf-Koeman for administrative assistance. This study was supported in part by Dutch Heart Association Grant 92.305.

REFERENCES

1. Gajewski TF, Schell SR, Nau G, Fitch FW. Regulation of T-cell activation: differences among T-cell subsets. *Immunol Rev* 1989;111:79–109.
2. Butcher EC, Picker LJ. Lymphocyte homing and homeostasis. *Science* 1996;272:60–66.
3. Lichtman AH, Abbas AK. T-cells subsets: recruiting the right kind of help. *Curr Biol* 1997;7:R242–244.
4. Mukherji B, Arnbjarnarson O, Spitznagle LA, et al. Imaging pattern of previously in vitro sensitized and interleukin-2 expanded autologous lymphocytes in human cancer. *Nucl Med Biol* 1988;15:419–427.
5. Kuyama J, McCormick A, George AJT, et al. Indium-111 labelled lymphocytes isotope distribution and cell division. *Eur J Nucl Med* 1997;24:488–496.
6. Botti C, Negri DRM, Seregni E, et al. Comparison of three different methods for radiolabelling human activated T lymphocytes. *Eur J Nucl Med* 1997;24:497–504.
7. Thakur ML, Marcus C, Huynh TV, et al. Imaging rheumatoic joint disease with anti-T-lymphocytes antibody OKT-3. *Nucl Med Commun* 1994;15:824–830.
8. Heinel LA, Rubin S, Rosenwasser RH, Vasthare US, Tuma RF. Leukocyte involvement in cerebral infarct generation after ischemia and reperfusion. *Brain Res Bull* 1994;34:137–141.
9. Holda JH, Swanborg RH. Autoimmune effector cells: II. Transfer of experimental allergic encephalomyelitis with a subset of T-lymphocytes. *Eur J Immunol* 1982;12:453–455.
10. Jander S, Kraemer M, Schroeter M, Witte OW, Stoll G. Lymphocytic infiltration and expression of intercellular adhesion molecule-1 in photochemically induced ischemia of the rat cortex. *J Cereb Blood Flow Metab* 1995;15:42–51.
11. Martino G, Clementi E, Brambilla E. Interferon activates a previously undescribed Ca^{2+} influx in T lymphocytes from patients with multiple sclerosis. *Proc Natl Acad Sci USA* 1994;91:4825–4829.
12. Martino G, Filippi M, Martinelli V, Brambilla E, Comi G, Grimaldi LME. Clinical and radiologic correlates of a novel T lymphocyte γ-interferon-activated Ca^{2+} influx in patients with relapsing-remitting multiple sclerosis. *Neurology* 1996;46:1416–1421.
13. Bekerman C, Nayak SM. Gallium imaging. In: Henkin RE, Boles MA, Karesh SM, et al., eds. *Nuclear medicine*. St. Louis, MO: Mosby YearBook; 1996:1597–1618.
14. Callahan RJ, Ramberg KL. Radiolabeling formed elements of blood: methods and mechanisms. In: Henkin RE, Boles MA, Karesh SM, et al., eds. *Nuclear medicine*. St. Louis, MO: Mosby YearBook; 1996:397–409.
15. Coleman RE, Datz FL. Detection of inflammatory disease using radiolabeled cells. In: Sandler MP, Patton JA, Coleman RE, Gottschalk A, Wackers FJTh, Hofferm PB, eds. *Diagnostic nuclear medicine*, 3rd ed. Baltimore: Williams and Wilkins; 1996:1509–1524.
16. Forstom L. Indium-111 labeled leukocyte imaging in the diagnosis of infaction and inflammatory disease. In: Henkin RE, Boles MA, Karesh SM, et al., eds. *Nuclear medicine*. St. Louis, MO: Mosby Yearbook; 1996:1619–1635.
17. Neumann RD, McAfee JG. Gallium-76 imaging in infection. In: Sandler MP, Patton JA, Coleman RE, Gottschalk A, Wackers FJTh, Hofferm PB, eds. *Diagnostic nuclear medicine*, 3rd ed. Baltimore: Williams and Wilkins; 1996;1493–1507.
18. Peters AM. Imaging inflammation and inflection with ^{99m}Tc HMPAO labeled leukocytes. In: Henkin RE, Boles MA, Karesh SM, et al., eds. *Nuclear medicine*. St. Louis, MO: Mosby Yearbook; 1996:1636–1655.
19. Melder RJ, Elmaleh D, Brownell AL, Brownell GL, Jain RK. A method for labeling cells for positron emission tomography (PET) studies. *J Immunol Meth* 1994;175:79–87.
20. Jansen HML, Pruim J, Van der Vliet AM, et al. Visualization of damaged brain tissue after ischemic stroke with ^{55}Co positron emission tomography. *J Nucl Med* 1994;35:456–460.
21. Jansen HML, Pruim J, Paans AMJ, et al. Visualization of ischemic brain damage with ^{55}Co positron emission tomography in man. *J Cereb Blood Flow Metab* 1993;13(suppl):S707–S708.
22. Jansen HML, Paans AMJ, Van der Vliet AM, et al. Cobalt-55 positron emission tomography in ischemic stroke. *Clin Neurol Neurosurg* 1997;99:6–10.
23. Jansen HML, Van der Naalt J, Van Zomeren AH, et al. Cobalt-55 positron emission tomography in traumatic brain injury: a pilot study. *J Neurol Neurosurg Psychol* 1996;60:221–223.
24. Jansen HML, Willemsen ATM, Sinnige LGF, et al. Cobalt-55 positron emission tomography in relapsing-progressive multiple sclerosis. *J Neurol Sci* 1995;132:139–145.
25. Joosten AAJ, Jansen HML, Piers A, Minderhoud JM, Korf J. Cobalt-57 SPECT in relapsing-progressive multiple sclerosis: a pilot study. *Nucl Med Commun* 1995;16:703–705.
26. Stevens H, Jansen HML, DeReuck J, Korf J. Imaging of stroke. In: Ter Horst GJ, Korf J, eds. *Clinical pharmacology of cerebral ischemia*. Totowa, NJ: Humana Press; 1997:31–42.
27. Gramsbergen JBP, Veenma-van der Duin L, Loopuijt LD, Paans AMJ, Vaalburg W, Korf J. Imaging of the degeneration of neurons and their processes in rat or cat brain by $^{45}CaCl_2$ autoradiography or $^{55}CoCl_2$ positron emission tomography. *J Neurochem* 1988;50:1798–1807.
28. Jansen HML, Knollema S, Veenma-van der Duin L, et al. Pharmacokinetics and dosimetry of 55- and 57-cobalt chloride. *J Nucl Med* 1996;37:2082–2087.
29. Pressman BC. Biological applications of ionophores. *Ann Rec Biochem* 1976;45:501–532.
30. Osman S, Danpure HJ. Fluorine-18-2-fluorodeoxy-D-glucose (18-FDG) labelling of human granulocytes to study inflammation by positron emission tomography (PET) [Abstract]. *Eur J Nucl Med* 1989;15:577.
31. Weiss A, Wiskocil RL, Stobo JD. The role of T3 surface molecules in the activation of human T cells: a two-stimulus requirement for Il-2 production reflects events occurring at a pre-translational level. *J Immunol* 1984;133:123–128.
32. Polman CH, Matthaei I, de Groot CJA, Koetsier JC, Sminia T, Dijkstra C. Low-dose cyclosporin A induces relapsing remitting experimental allergic encephalomyelitis in the Lewis rat. *J Neuroimmunol* 1988;17:209–216.
33. Wang P-Y, Kao C-H, Mui M-Y, Wang S-J. Leukocyte infiltration in acute hemispheric ischemic stroke. *Stroke* 1993;24:236–240.
34. Wekerle H. Lymphocyte traffic to the brain. In: Pardridge WA, ed. *Blood brain barrier*. New York: Raven Press; 1993;67–81.